

# A Low-Complexity Solution to Angular Misalignments in Molecular Index Modulation

Ahmet Celik\*, Mustafa Can GURSOY<sup>†</sup>, Ertugrul Basar<sup>‡</sup>, Ali Emre Pusane<sup>†</sup>, Tuna Tugcu\*\*

\*Department of Electronics and Communications Engineering, Istanbul Technical University, Istanbul, Turkey

<sup>†</sup>Department of Electrical and Electronics Engineering, Bogazici University, Istanbul, Turkey

<sup>‡</sup>Department of Electrical and Electronics Engineering, CoreLab, Koç University, Istanbul, Turkey

\*\*Department of Computer Engineering, NETLAB, Bogazici University, Istanbul, Turkey

E-mail: celikahme@itu.edu.tr, {can.gursoy, ali.pusane, tugcu}@boun.edu.tr, ebasar@ku.edu.tr

**Abstract**—Multiple-input multiple-output (MIMO) transmission approaches have been recently considered in the context of molecular communications due to desirable improvements they provide in terms of communication efficiency. Among these methods, molecular index modulation (molecular-IM) schemes yield a significant improvement in throughput and show promising results for future molecular MIMO research. However, existing molecular-IM methods rely on perfect spatial alignment between corresponding antennas, which may not be the case in a possible practical scenario. Motivated by this practical constraint, this study proposes a novel receiver design for molecular-IM. The proposed decoder is an augmented version of the maximum count decoder (MCD) and operates by merging MCD with a simple linear combining technique. Our numerical results show that the proposed approach yields a desirable robustness against antenna misalignments while still maintaining a simplistic receiver structure.

**Index Terms**—Molecular communications, index modulation, molecular MIMO, robust receiver design, antenna misalignment.

## I. INTRODUCTION

Molecular communication via diffusion (MCvD) transfers information by utilizing the diffusion mechanism [1]. In an MCvD system, the transmitter (TX) encodes the information in a physical property of the carrier molecules and emits them into the fluid communication environment where they can freely diffuse. At the receiver (RX) side, these molecules are collected, counted, and used to decode the transmitted information [2]. After their release, the emitted molecules exhibit Brownian motion in the channel, which introduces randomness to their arrivals at the RX end. This randomness causes some molecules to arrive at the RX after taking longer paths and this introduces inter-symbol interference (ISI) to an MCvD system and hinders high data rates [3].

Inspired by their desirable properties when applied to traditional wireless communications, multiple-input multiple-output (MIMO) transmission approaches are also proposed to molecular communications. When the MCvD system is considered to have multiple TX and RX antennas, such as in a molecular MIMO setting,

the question of how to utilize these resources arises. As candidate methods for molecular MIMO, the authors of [4] propose a space-time block code similar to the Alamouti approach and the repetition coding scheme in the spatial domain. In addition, pairing each TX and RX antenna, and providing spatial multiplexing (SMUX) by transmitting parallel and independent streams is also considered in [5]–[7]. SMUX shows significant resistance to ISI since it can satisfy a certain data rate while emitting molecules at a lower frequency. However, since the Brownian motion mechanism makes it highly likely for some molecules to arrive at unintended RX antennas, it suffers from severe inter-link interference (ILI).

Recently, the index modulation (IM), which is a popular and promising physical-layer concept for radio frequency (RF) communications [8], [9], is introduced to molecular MIMO communications [10]. It is found that molecular-IM schemes yield desirable error performance when communicating at higher data rates due to their strong ILI and ISI combating capabilities. In its general sense, molecular-IM considers encoding information in the index of the emitting antenna of a molecular MIMO system, rather than providing spatial multiplexing or transmitting space-time block codes. These spatial constellations may be accompanied by signal constellations that are molecule type-based [10], concentration-based [11], and pulse-position-based [12]. As in the molecular space shift keying (MSSK) scheme proposed by [10], the information can also be encoded solely on the spatial domain. Overall, molecular-IM methods can be used whenever a molecular MIMO setting is available and yield very promising results in terms of utilizing the increased device complexity due to the MIMO configuration, more efficiently.

As also used in [10], the maximum count decoder (MCD) can be utilized to decode the activated antenna in a molecular-IM scheme. MCD performs a simple comparison among arrival counts to decode the activated antenna and is a desirable decoding method due to its simplicity. However, the key problem with MCD is that it relies on each TX antenna and its corresponding RX

antenna to be perfectly aligned, and faces a performance degradation otherwise. Unfortunately, the perfect alignment assumption may not hold in both macro-scale and nano-scale applications. Motivated by this critical shortcoming of MCD, this study proposes a novel low-complexity decoding method to detect the activated antenna of a molecular-IM scheme in the presence of angular misalignments. The proposed scheme utilizes the availability of the channel impulse response (CIR) at the receiver end, and performs a linear diversity combining operation in conjunction with MCD to decode the activated antenna. Overall, our results show that even though it performs slightly worse than pure MCD at the perfect alignment scenario for some channel parameters, the proposed approach yields a desirable robustness against possible angular misalignments while still maintaining the low computational complexity of MCD-based detection schemes.

The rest of the paper is organized as follows: Section II discusses and demonstrates the adopted molecular MIMO system model while detailing the channel model of the system at hand. Section III introduces the proposed low-complexity receiver design. The numerical results and related discussion is provided in Section IV. Section V concludes the paper.

## II. SYSTEM MODEL

The system model consists of a single TX and a single RX unit in an unbounded, three dimensional diffusion channel, similar to the model considered in [10]. The fluid medium is homogeneous, driftless, and has a diffusion coefficient  $D$  for the messenger molecules. The TX unit has  $n_{TX}$  transmit antennas on its surface, which are point sources that can emit the messenger molecules to the medium. On the surface of the RX unit, there are  $n_{RX}$  absorbing receiver antennas that are spherical in shape with radius  $r_r$ . Throughout the paper,  $i^{th}$  TX antenna is referred to as  $TX_i$ , where  $i \in \{1, 2, \dots, n_{TX}\}$ . Similarly, the  $j^{th}$  RX antenna is referred to as  $RX_j$  where  $j \in \{1, 2, \dots, n_{RX}\}$ .  $n_{TX} = n_{RX} = 8$  is chosen in this paper. Other than the antennas on their respective surfaces, the TX unit's body is assumed to be transparent to the molecules whilst the RX unit's body elastically reflects them, similar to the system model adopted in [10].

The facing surfaces of the TX and RX units are parallel to each other and are separated with distance  $d_{TX-RX}$ . On their respective surfaces, TX and RX antennas are placed in a uniform circular array (UCA) formation [13]. Recalling that  $n_{TX} = n_{RX} = 8$  is considered in this paper, the angular separation between antennas in the UCA is  $\frac{\pi}{4}$ . It should be noted that the presented approach in this study is also applicable to  $n_{TX}$  &  $n_{RX}$  values other than 8 and antenna placements other than UCA. The choices of UCA and  $n_{TX} = n_{RX} = 8$  are solely for demonstrative purposes and are selected as

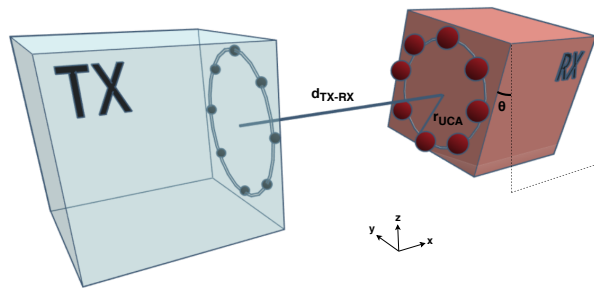


Fig. 1. The system model of interest for  $n_{TX} = n_{RX} = 8$ . Since the RX antennas are spherical, the distance between the center of the RX UCA and the projection of an RX antenna on the RX unit's surface becomes  $r_{UCA} - r_r$ . For the case of perfect alignment, the closest distance between a TX antenna and its corresponding RX antenna is  $d_{TX-RX} - 2r_r$ .

such in order for the work in this paper to be comparable to our earlier benchmark study [10].

In the system of interest, corresponding TX and RX antennas are assumed to be communicating pairs, and in an ideal scenario, each pair is perfectly aligned. However, in more practical scenarios, establishing an ideal alignment is a difficult task since TX and RX nanomachines are considered to be in a liquid medium. In this study, the circular rotation of concentric TX and RX units in the  $yz$ -plane is considered. Note that even though the communication environment is assumed to be quasi-static during the communication process, such a topology leads to an angular misalignment between corresponding antennas. Overall, denoting the angular misalignment between the concentric TX and RX UCA as  $\theta$ , the considered system model is as demonstrated in Fig. 1.

In a fluid MCvD channel, the messenger molecules emitted from TX antennas propagate randomly in all three spatial dimensions due to the nature of Brownian motion. This behavior of the molecules is modeled with a random-walk process in each dimension for each discrete time step  $\Delta t$  [1]. In this paper, the CIR is generated via particle-based Monte Carlo simulations (similar to [10]) using  $10^6$  molecules for each scenario and with an incremental time step of  $\Delta t = 10^{-4}$ s. The obtained CIR is utilized to find the channel coefficients for the time-slotted MIMO MCvD system's characterization. The  $n^{th}$  channel coefficient between  $TX_i$  and  $RX_j$  is denoted by  $h_{i,j}[n]$ .

The channel coefficient  $h_{i,j}[n]$  corresponds to the probability of a single molecule that is transmitted from  $TX_i$  to arrive at  $RX_j$  in time slot  $n$ . In scenarios where multiple molecules are transmitted from  $TX_i$ , the received number of molecules at  $RX_j$  in time slot  $n$  can be approximated to follow independent binomial distributions with success probability  $h_{i,j}[n]$  [6]. As also pointed out by [14], the binomial arrivals can be approximated as Gaussian distributions in MCvD, as

well. Overall, the arrival count at  $RX_j$  during symbol interval  $n$  can be shown as  $R_j[n] \sim \mathcal{N}(\mu_j[n], \sigma_j^2[n])$ . Here, the mean of the distribution is found by

$$\mu_j[n] = \sum_{z=n-L+1}^n \sum_{i=1}^{n_{TX}} s_i[z] h_{i,j}[n-z+1] \quad (1)$$

and the variance by

$$\sigma_j^2[n] = \sum_{z=n-L+1}^n \sum_{i=1}^{n_{TX}} s_i[z] h_{i,j}[n-z+1] (1 - h_{i,j}[n-z+1]). \quad (2)$$

Here,  $s_i[z]$  denotes the number of transmitted molecules from  $TX_i$  at the  $z^{th}$  time slot, and  $L$  denotes the considered channel memory. In order to sufficiently capture the heavy right tail of the arrival distribution,  $L = 30$  is considered in this paper.

### III. PROPOSED METHOD

The MSSK scheme introduced in [10] encodes the information solely in the spatial domain. That is to say, each antenna index represents a symbol in MSSK and the transmission is performed over the appropriate antennas according to the symbol sequence to be sent. At every transmission instant,  $\log_2 n_{TX}$  bits are grouped and mapped into an MSSK symbol, which leads to an emission from the activated antenna. Note that only one TX antenna is active at a time for MSSK, meaning all TX antennas other than the activated one are silent for each transmission.

The molecules are released at the beginning of each time slot from the TX unit's activated antenna. Assuming that the RX can be synchronized in time with the TX [15], the RX counts the molecules that arrive at its antennas until the end of the time slot. The MSSK symbol is then decoded via the MCD by comparing the number of arrival counts to each RX antenna. The corresponding TX antenna of the RX antenna with the maximum molecule count is detected to be active and said TX antenna's index is decoded as the received symbol. Denoting  $\mathbf{x}[k]$  as the activated antenna index at the  $k^{th}$  instant and  $\hat{\mathbf{x}}[k]$  as the decoded antenna index, the MCD's operation can be expressed as

$$\hat{\mathbf{x}}[k] = \arg \max_{j \in [1, \dots, n_{RX}]} R_j[k]. \quad (3)$$

The MSSK scheme is shown to yield a reliable error performance when used in conjunction with MCD [10]. In addition, MCD is a very simple and memoryless decoder that be implemented with a single comparator circuit. However, one shortcoming of MCD is that it assumes the perfect alignment of corresponding TX and RX antennas. Unfortunately, possible misalignments may occur in more practical scenarios, which degrades MCD's overall performance. Motivated by this issue,

we propose a linear diversity combiner in order to increase the robustness in these scenarios. The core of the proposed combining operation is an element-wise multiplication of the received molecule vector with a diversity combining vector, which is referred to as  $\mathbf{v}$  throughout the paper. Denoting  $R_j[k]$  as the arrival to  $RX_j$  at the  $k^{th}$  time slot, the combination operation can be denoted as

$$R'_j[k] = \sum_{j=1}^{n_{TX}} (\mathbf{r}[k] \circ \mathbf{v}_j)_j. \quad (4)$$

Here,  $\mathbf{r}[k]$  is the arrival vector at the  $k^{th}$  time slot,  $\circ$  represents the element-wise multiplication operation, and  $(\cdot)_j$  denotes the  $j^{th}$  element in its argument vector. In addition,  $\mathbf{v}_j$  denotes the combining vector that corresponds to  $RX_j$ .

In order to combat with the misalignment problem, it is assumed that CIR can be estimated at the RX unit by using a method similar to [16] under the quasi-static channel assumption. Using the availability of CIR, we have heuristically chosen the  $\mathbf{v}_j$  vector as

$$\mathbf{v}_j = [h_{j,1}[1] \quad h_{j,2}[1] \quad \dots \quad h_{j,n_{RX}}[1]]^T, \quad (5)$$

which is equal to the first channel coefficient resulting from a transmission by  $TX_j$ . Note that since the UCA topology provides spatial symmetry, the combining vector that corresponds to  $RX_j$  can be simply obtained by

$$\mathbf{v}_j = [\mathbf{v}_1]_{j-1}, \quad (6)$$

where  $[\mathbf{v}_1]_{j-1}$  denotes the  $(j-1)^{th}$  cyclic shift of the original  $\mathbf{v}_1$  vector. Following the selection of the  $\mathbf{v}$  vectors as (5) and performing the diversity combining operation as (4), the proposed decoder employs the  $\arg \max$  operation described in (3) as the last step to detect the MSSK symbol. Note that once the CIR is estimated, the proposed approach is a very low-complexity method, employing only  $n_{RX}$  calls to the linear diversity combining operation defined in (4). Overall, Algorithm 1 describes the operations that constitute the proposed receiver design.

It is worth emphasizing that the UCA topology provides simplifications due to the spatial symmetry it provides and allows an easy derivation for  $\mathbf{v}_j$  when  $j \neq 1$ . However, even though this topological property is utilized for obtaining the combining vector in a simpler form, the approach for finding  $\mathbf{v}_j$  is proposed in a generalized manner for all antenna topologies in (5), rather than specifically for the UCA topology. In addition, the proposed diversity combining-based receiver design is presented by its application on MSSK but it can be adapted to any molecular-IM scheme where the antenna index is being decoded. Such schemes may include the molecular spatial modulation (MSM) in [10], concentration-based spatial modulation in [11], pulse

**Algorithm 1** Receiver operations for the proposed method.

**Inputs:**  $t_b, M, n_{TX}, n_{RX}, s_T, \mathcal{L}$

- 1:  $M$ : Molecule budget to transmit a single bit
- 2:  $t_b$ : Bit duration
- 3:  $n_{TX}$  &  $n_{RX}$ : Number of TX & RX antennas
- 4:  $s_T$ : Training sequence for channel estimation ([16])
- 5:  $\mathcal{L}$ : Length of the symbol sequence

**Output:** Decoded antenna index sequence ( $\hat{\mathbf{x}}$ )

- 6: Symbol duration  $t_s = \log_2(n_{TX})t_b$
- 7: Estimate channel coefficients  $h_{i,j}[n]$  using  $s_T$  ([16])
- 8: **for**  $j = 1$  to  $n_{RX}$  **do**
- 9:      $\mathbf{v}_j = [h_{j,1}[1] \quad h_{j,2}[1] \quad \dots \quad h_{j,n_{RX}}[1]]^T$
- 10: **end for**
- 11: Data communication begins.
- 12: **for**  $k = 1$  to  $\mathcal{L}$  **do**
- 13:     Count molecule arrivals in  $t \in [(k-1)t_s, kt_s]$  for all antennas to find  $R_j[k], j = 1, \dots, n_{RX}$
- 14:      $\mathbf{r}[k] = [R_1[k] \quad R_2[k] \quad \dots \quad R_{n_{RX}}[k]]$
- 15:      $R'_j[k] = \sum_{j=1}^{n_{TX}} (\mathbf{r}[k] \circ \mathbf{v}_j)_j$
- 16:      $\hat{\mathbf{x}}[k] = \arg \max_{j \in \{1, \dots, n_{RX}\}} R'_j[k]$
- 17: **end for**
- 18: **return**  $\hat{\mathbf{x}}$

position-based molecular spatial modulation in [12], and possibly more.

#### IV. NUMERICAL RESULTS

In this section, symbol error rate (SER) performances of the conventional MCD and our proposed approach are comparatively analyzed through computer simulations for 8-MSSK. To observe the contribution of our approach in the presence of angular misalignments, the evaluations are presented for  $\theta = \frac{\pi}{32}, \frac{\pi}{24}, \frac{\pi}{16}$ , and  $\frac{\pi}{8}$  radians. Note that, since a UCA setting with  $n_{TX} = n_{RX} = 8$  and an angular separation of  $\frac{\pi}{4}$  is considered in this paper,  $\theta$  values larger than  $\frac{\pi}{8}$  can be equivalently represented by a value smaller than  $\frac{\pi}{8}$ . For example,  $\theta = \frac{3\pi}{16}$  is equivalent to  $\frac{\pi}{16}$  for our system of interest. Lastly,  $\theta = 0$  is also considered as it corresponds to the perfectly aligned system.

The parameters used in the performed computer simulations are presented in Table I. Here,  $M$  stands for the number of transmitted molecules per bit,  $t_b$  represents the bit duration (reciprocal of the bit rate) of

TABLE I  
SYSTEM AND CHANNEL PARAMETERS. DEFAULT VALUES ARE SHOWN IN BOLD.

Parameter	Value
$M$ (molecules)	50, 100, <b>150</b> , 200, 250
$t_b$ (s)	0.2, <b>0.3</b> , 0.4, 0.5
$r_{UCA}$ ( $\mu\text{m}$ )	<b>15</b> , 17.5, 20, 22.5
$d_{TX-RX}$ ( $\mu\text{m}$ )	20
$D$ ( $\frac{\mu\text{m}^2}{\text{s}}$ )	79.4
$r_r$ ( $\mu\text{m}$ )	5
$L$ (memory slots)	30

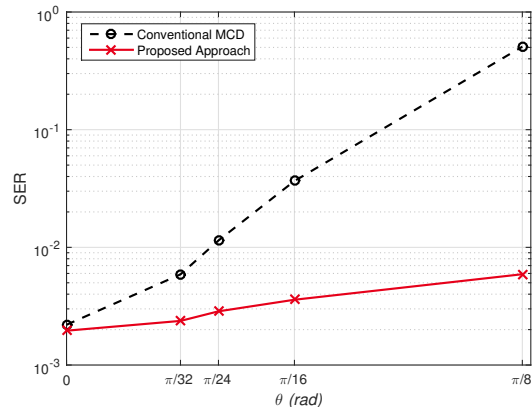


Fig. 2. SER vs.  $\theta$  curves for conventional MCD and the proposed method.  $M = 150$  molecules,  $t_b = 0.3\text{s}$ ,  $r_{UCA} = 15\mu\text{m}$ ,  $d_{TX-RX} = 20\mu\text{m}$ ,  $D = 79.4\mu\text{m}^2/\text{s}$ ,  $r_r = 5\mu\text{m}$ , and  $L = 30$ .

the communication link, and  $r_{UCA}$  denotes the radii of the TX and RX UCA. Utilizing the default parameters, which are shown with **boldface** text in Table I, Fig. 2 is presented to comparatively demonstrate the SER performances of the proposed scheme and conventional MCD under varying  $\theta$ .

It can be observed from Fig. 2 that conventional MCD is harshly affected from an angular misalignment. As also mentioned in Section III, MCD is designed for the  $\theta = 0$  (perfect alignment) case, and it assumes that  $RX_j$  is expected to absorb the largest number of molecules when a transmission is made from  $TX_j$ . Note that, since a misalignment in the system increases the expected arrival count at an adjacent RX antenna and decreases the expected arrivals at the intended RX antenna, MCD's performance deteriorates. In the extreme case of  $\theta = \frac{\pi}{8}$ , two RX antennas are equidistant from each TX antenna, which suggests equal expected arrivals at these antennas and renders the MCD useless. On the other hand, the proposed method weighs the arrivals at the RX antennas according to their channel coefficients before combining, thus mitigating the negative effect of: i) a possible decrease in the expected arrival at the intended antenna, ii) a possible increase in the expected arrival rate at the adjacent antenna. By doing so, it can be observed from Fig. 2 that the proposed method is able to yield an acceptable error performance even for the most extreme misalignment scenario of  $\theta = \frac{\pi}{8}$ .

The effect of  $M$  on the SER performance of conventional MCD and the proposed method is presented in Fig. 3 where overall SER decreases with increasing  $M$ , which is a well-known phenomenon in the molecular communications literature. Since (1) and (2) suggest that both means and variances of the arrival distributions are directly proportional to the transmitted number of molecules, it can be inferred that the mean over standard deviation ratio ( $\frac{\mu_j[k]}{\sigma_j[k]}$ ) improves with increasing  $M$ . The

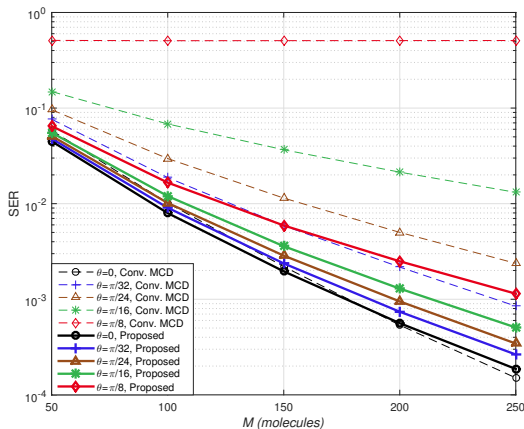


Fig. 3. SER vs.  $M$  curves for conventional MCD and the proposed method.  $t_b = 0.3s$ ,  $r_{UCA} = 15\mu m$ ,  $d_{TX-RX} = 20\mu m$ ,  $D = 79.4 \mu m^2/s$ ,  $r_r = 5\mu m$ , and  $L = 30$ .

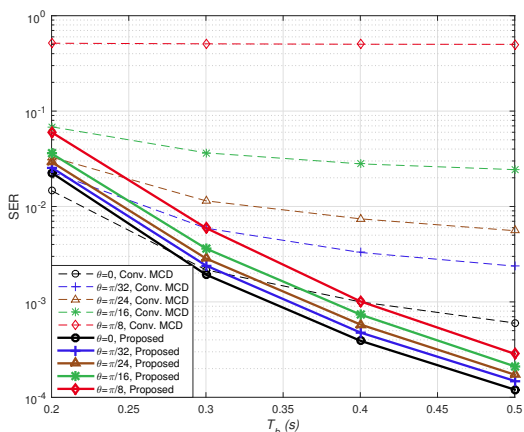


Fig. 4. SER vs.  $t_b$  curves for conventional MCD and proposed method.  $M = 150$  molecules,  $r_{UCA} = 15\mu m$ ,  $d_{yz} = 15\mu m$ ,  $D = 79.4 \mu m^2/s$ ,  $r_r = 5\mu m$ , and  $L = 30$ .

improved  $\frac{\mu_j[k]}{\sigma_j[k]}$  ratio results in a lower relative arrival noise, hence decreases the error rate for all scenarios. However, Fig. 3 shows that the downward slope of the SER vs.  $M$  curve is better protected with the proposed approach under varying  $\theta$ , as the curves for different  $\theta$  values are more tightly packed than the curves for conventional MCD.

The comparative SER performances of the proposed method and the conventional MCD on 8-MSSK under varying bit durations ( $t_b$ ) are presented in Fig. 4. It can be observed from Fig. 4 that for  $t_b = 0.2s$ , the proposed method improves the SER performance for misaligned channels, while sacrificing from the performance on the perfectly aligned scenario by a small margin. However, as the  $t_b$  constraint is relaxed, the proposed method strictly outperforms conventional MCD.

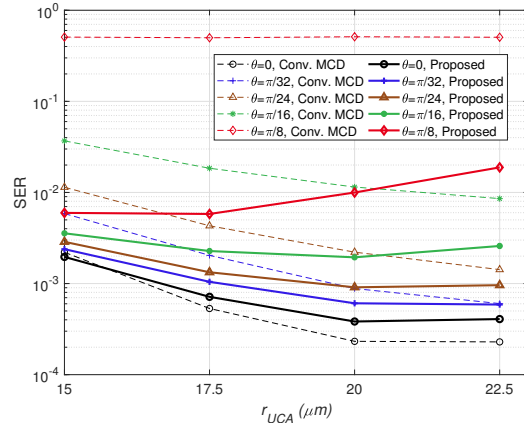


Fig. 5. SER vs.  $d$  curves for conventional MCD and proposed method.  $M = 150$  molecules per bit,  $t_b = 0.3s$ ,  $r_{UCA} = 15\mu m$ ,  $d_{yz} = 15\mu m$ ,  $D = 79.4 \mu m^2/s$ ,  $r_r = 5\mu m$ , and  $L = 30$ .

As also shown by [10], increasing  $t_b$  results in an ILI-dominated channel since ISI decreases and ILI increases with  $t_b$ . Therefore, it can be inferred from Fig. 4 that diversity combining may be utilized for ILI reduction in molecular-IM schemes.

Fig. 5 shows the effect of varying  $r_{UCA}$  on the SER performance of 8-MSSK when employed in conjunction with the proposed approach and conventional MCD. It can be observed from Fig. 5 that the radius of the UCA has an interesting effect on SER. Up to a certain point, an increase in  $r_{UCA}$  results in the improvement in the SER performance for most of the channels. This relationship is mainly due to the ILI reduction introduced by the increase in antenna separation. However, as also reported by [10], a wider antenna separation increases ISI. Since all RX antennas are absorbing, they remove the molecules from the medium and prevent them from reaching another RX antenna in following time slots [17]. In a molecular MIMO system, this behavior reduces ISI and is a very desirable trait of the MIMO setting in molecular communications. Increasing antenna separation reduces this beneficial ISI mitigation ability of RX antennas, posing a trade-off between the ISI and ILI faced by a molecular MIMO system. Such a trade-off suggests the existence of an optimum  $r_{UCA}$  value that obtains the best SER performance.

Overall, Fig. 5 shows that the proposed approach provides its desirable performance gain for different  $r_{UCA}$  values, as well. Furthermore, the fact that the performance gap is larger in favor of the proposed approach for smaller  $r_{UCA}$  values supports our claim that diversity combining is a promising approach for ILI combating for molecular-IM.

## V. CONCLUSION

In this study, we have introduced a novel decoder for the MSSK scheme that is more robust to angular

misalignments between TX and RX antennas. We have shown through computer simulations that our approach yields a desirable error performance whilst still conserving the advantage of MCD-based decoders regarding the computational complexity. One thing to note is that the introduced decoder is heuristically proposed, which hints towards further possible performance enhancement with different designs. The development of other and possibly more robust diversity combining strategies are left as a future work. Possible future work also includes the analysis of other misalignments such as azimuthal shifts and non-concentric alignments, which were not included in the study.

#### ACKNOWLEDGEMENTS

This work was partially supported by State Planning Organization of Turkey (DPT) under grant number DPT-2007K120610. The work of E. Basar was supported by the Turkish Academy of Sciences GEBIP Programme.

#### REFERENCES

- [1] T. Nakano, A. W. Eckford, and T. Haraguchi, *Molecular communication*. Cambridge University Press, 2013.
- [2] I. F. Akyildiz, F. Brunetti, and C. Blzquez, "Nanonetworks: A new communication paradigm," *Comput. Netw.*, vol. 52, no. 12, pp. 2260 – 2279, Aug. 2008.
- [3] N. Farsad, H. B. Yilmaz, A. Eckford, C. B. Chae, and W. Guo, "A comprehensive survey of recent advancements in molecular communication," *IEEE Commun. Surveys Tuts.*, vol. 18, no. 3, pp. 1887–1919, Feb. 2016.
- [4] M. Damrath, H. B. Yilmaz, C. Chae, and P. A. Hoeher, "Array gain analysis in molecular MIMO communications," *IEEE Access*, vol. 6, pp. 61 091–61 102, Oct. 2018.
- [5] L. S. Meng, P. C. Yeh, K. C. Chen, and I. F. Akyildiz, "MIMO communications based on molecular diffusion," in *Proc. IEEE Global Commun. Conf. (GLOBECOM)*, Dec. 2012, pp. 5380–5385.
- [6] B. H. Koo, C. Lee, H. B. Yilmaz, N. Farsad, A. Eckford, and C.-B. Chae, "Molecular MIMO: From theory to prototype," *IEEE J. Sel. Areas Commun.*, vol. 34, no. 3, pp. 600–614, Mar. 2016.
- [7] B. H. Koo, H. B. Yilmaz, C. B. Chae, and A. Eckford, "Detection algorithms for molecular MIMO," in *Proc. 2015 IEEE Intl. Conf. on Commun. (ICC)*, June 2015, pp. 1122–1127.
- [8] E. Basar, "Index modulation techniques for 5G wireless networks," *IEEE Commun. Mag.*, vol. 54, no. 7, pp. 168–175, July 2016.
- [9] E. Basar, M. Wen, R. Mesleh, M. Di Renzo, Y. Xiao, and H. Haas, "Index modulation techniques for next-generation wireless networks," *IEEE Access*, vol. 5, pp. 16 693–16 746, Aug. 2017.
- [10] M. C. Gursoy, E. Basar, A. E. Pusane, and T. Tugcu, "Index modulation for molecular communication via diffusion systems," *IEEE Trans. Commun.*, vol. 67, no. 5, pp. 3337–3350, May 2019.
- [11] Y. Huang, M. Wen, L.-L. Yang, C.-B. Chae, and F. Ji, "Spatial modulation for molecular communication," *arXiv preprint arXiv:1807.01468*, July 2018.
- [12] M. C. Gursoy, E. Basar, A. E. Pusane, and T. Tugcu, "Pulse position-based spatial modulation for molecular communications," *IEEE Commun. Lett.*, vol. 23, no. 4, pp. 596–599, Apr. 2019.
- [13] C. A. Balanis, "Antenna theory: A review," *Proc. IEEE*, vol. 80, no. 1, pp. 7–23, Jan. 1992.
- [14] H. B. Yilmaz, C.-B. Chae, B. Tepekule, and A. E. Pusane, "Arrival modeling and error analysis for molecular communication via diffusion with drift," in *Proc. ACM 2nd Ann. Int. Conf. on Nanoscale Comput. and Commun.*, Sep. 2015.
- [15] M. J. Moore and T. Nakano, "Oscillation and synchronization of molecular machines by the diffusion of inhibitory molecules," *IEEE Trans. Nanotechnol.*, vol. 12, no. 4, pp. 601–608, July 2013.
- [16] S. M. Rouzgar and U. Spagnolini, "Channel estimation for diffusive MIMO molecular communications," in *Proc. European Conf. on Netw. and Commun. (EuCNC)*, June 2017, pp. 1–5.
- [17] S. S. Assaf, S. Salehi, R. G. Cid-Fuentes, J. Solé-Pareta, and E. Alarcón, "Influence of neighboring absorbing receivers upon the inter-symbol interference in a diffusion-based molecular communication system," *Nano Commun. Netw.*, vol. 14, pp. 40–47, Dec. 2017.